Prepared for:

Rijkswaterstaat, RIKZ

Yearly averaged sediment transport along the Dutch shore

Upgrading of UNIBEST-TC

April 1995

H 2129 - 1

delft hydraulics

Yearly averaged sediment transport along the Dutch shore

Upgrading of UNIBEST-TC

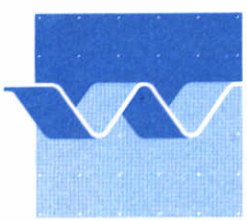

delft hydraulics

Contents

1 Introduction

In a study for RIKZ (DELFT HYDRAULICS report H1887) to predict the yearly averaged longshore sediment transport along the closed part of the Dutch shore, the predictions obtained at the 20 and 8 m depth contour differ considerably from the results obtained for a similar study carried out in 1989 ("Kustverdedigingsnota"). One of the goals of the newly performed sediment transport computations was to evaluate the results obtained for the previous prediction by implementing state of the art knowledge on hydrodynamics and morphology in a numerical model. Based on these results a recalibration of the previous computations would be enough to come up with improved predictions for the cross-shore distribution of the yearly averaged sediment transport rates. Because of the large differences found this recalibration is no longer possible and additional computations inside the surfzone are required to obtain the cross-shore distribution.

To compute the sediment transport rates inside the surfzone the UNIBEST-TC model is upgraded to the same level as the model used to evaluate the yearly averaged sediment transports at the 20 and 8 m water depth. The following model components, which have been upgraded are described in this report:

- wave propagation and dissipation,
- wave driven currents,
- wind driven currents,
- time series of the near-bed orbital velocity,
- bed-and suspended load sediment transport.

To check whether the upgraded formulations have been implemented correctly, some basic tests have been performed. In another study (H2130) parallel to this one, the upgraded model is validated against the data obtained during the LIP-11D Deltaflume tests performed in spring 1993. Here only some typical results obtained during this validation are presented to show that the model exhibits the correct behaviour.

Next the model was used to compute the cross-shore distribution of the yearly averaged sediment transport. The procedure, which is similar to the one used in previous computations (H1887), is treated in the last chapter. The resulting yearly-averaged sediment transports rates are used as part of the input for a model to predict the large scale coastal behaviour (Zandbalans). Therefore the resulting sediment transport rates are not included here, but will be treated as prt of that study.

The progress in the upgraded UNIBEST is summarized in the following points:

- roller contribution to the momentum balance,
- wind driven currents,
- an improved sediment transport formulation,
- an advanced parametrisation of the wave-current interaction,
- timeseries of near velocity.

2 Upgraded model formulations

2.1 Coordinate system

The x-axis is perpendicular to the shoreline, positive landwards.
The y-axis is rotated 90 degrees counter-clockwise.
All angles are expressed as angle, counterclockwise, from x-axis to direction of propagation.
In the computational part, *no transformations from or to an East/North system or a nautical system are carried out.*

2.2 Wave model

The wave propagation model consists of three first-order differential equations, viz. the time-averaged wave energy balance (Battjes and Janssen, 1978), the balance equation for the energy contained in surface rollers in breaking waves (Nairn et al., 1990) and the horizontal momentum balance from which the mean water level set-up is computed. The refraction of the waves is computed using Snel's law. The three coupled equations are solved by numerical integration over the cross-shore profile. These equations generate the input required by the local models for the vertical velocity profile, the concentration vertical and the bed-load transport.

2.2.1 Differential equations

The following coupled differential equations have to be solved for a given bottom profile:

Energy balance equation for the wave energy E:

$$\frac{\partial}{\partial x}\left(E\,C_g\cos\theta\right) = -D_w \tag{2.2.1}$$

Balance equation for the energy of rollers travelling on top of breaking waves:

$$\frac{\partial}{\partial x}\left(E_r\,C\cos\theta\right) = +D_w - Diss \tag{2.2.2}$$

Cross-shore momentum equation (set-up equation):

$$\frac{\partial\overline{\eta}}{\partial x} = -\frac{1}{\rho g h}\frac{\partial S_{xx}}{\partial x} \tag{2.2.3}$$

The unknown variables to be solved are E, E_r and $\overline{\eta}$, the wave energy, the roller energy and the set-up, respectively.

The wave energy balance is closed by the following relations:

$$D_w = \frac{1}{4}\rho g\,\alpha f_p H_{\max}^2 Q_b \tag{2.2.4}$$

where:

$$H_{max} = \frac{0.88}{k}\tanh\left(\frac{\gamma kh}{0.88}\right) \tag{2.2.5}$$

$$\gamma = 0.5 + 0.4\tanh(33 s_0) \tag{2.2.6}$$

Here, D_w is the dissipation of organised wave energy, s_0 is the deep water steepness $H_{rms,0}/L_0$, ρ is the density, g is the acceleration of gravity, α is a coefficient equal to 1, f_p is the peak frequency, H_{max} is the maximum wave height and Q_b is the fraction of breaking waves.

The roller energy balance is closed by the relation:

$$Diss = \beta g \frac{E_r}{C} \tag{2.2.7}$$

where $Diss$ is the total energy dissipation, β is a coefficient (0.05-0.10) and C is the wave propagation speed.

In the momentum balance, the radiation stress S_{xx} is related to the primary variables by:

$$S_{xx} = \left((2\frac{C_g}{C}\cos^2\theta - 0.5)E + E_r\cos\theta\right) \tag{2.2.8}$$

The local water depth h is defined as:

$$h = \overline{\eta} - z_b \tag{2.2.9}$$

where z_b is the bottom level relative to a reference plane.
The wave direction θ is defined as the angle between the x-axis (perpendicular to the shoreline, positive landwards) and the propagation direction, and is found from Snel's law:

$$\frac{\sin\theta}{\sin\theta_0} = \frac{C}{C_0} \tag{2.2.10}$$

where the subscript 0 refers to deep water values.

The propagation speed C is defined as

$$C = \omega/k \tag{2.2.11}$$

where $\omega = 2\pi f_p$ is the angular frequency, and k is the wave number, which is solved from the dispersion relation:

$$\omega^2 = gk\tanh(kh) \tag{2.2.12}$$

The system requires boundary conditions for E, E_r, $\overline{\eta}$ and θ and a bottom profile $z_b(x)$. Coefficient values must be given for α (default value 1), γ (default value given by equation 6) and β (optimum value between 0.05 and 0.10).

2.3 Mean current profile

For the computation of the mean current profile, we use an eddy viscosity model (zero equation turbulence model). Three layers are identified, cf. De Vriend and Stive (1987):

- the trough-to crest layer, which is represented by boundary conditions on the middle layer, applied at mean water level;
- the middle layer, from the top of the bottom (wave) boundary layer to the mean water level;
- the bottom boundary layer.

Different viscosity distributions are applied in the bottom layer and the middle layer. The assumed viscosity distribution in both layers is parabolic, and zero at $\sigma=0$. :

$$\nu_t = \phi_s \overline{\nu_t}\, \sigma(\sigma_s-\sigma) \qquad , \sigma>\delta \tag{2.3.1a}$$

$$\nu_t = \phi_s \overline{\nu_t}\, \sigma(\sigma_s-\sigma) + \phi_b \overline{\nu_{tb}}\, \sigma(\delta-\sigma)$$

$$= (\phi\nu)_b\, \sigma(\sigma_b-\sigma) \qquad , \sigma<\delta \tag{2.3.1b}$$

where: $\sigma = z/h$, the relative height above the bed; δ is the boundary layer thickness;

$$\phi_s^{-1} = \int_0^1 \sigma\,(\sigma_s-\sigma)\, d\sigma \tag{2.3.2}$$

$$\phi_b^{-1} = \int_0^\delta \sigma\,(\delta-\sigma)\, d\sigma \tag{2.3.3}$$

$$(\phi\nu)_b = \phi_s\overline{\nu_t} + \phi_b\overline{\nu_{tb}} \tag{2.3.4}$$

$$\sigma_b = \frac{\phi_s\overline{\nu_t}\sigma_s + \phi_b\overline{\nu_{tb}}\delta}{\phi_s\overline{\nu_t} + \phi_b\overline{\nu_{tb}}} \tag{2.3.5}$$

Momentum balance in i-direction, i= x or y

$$\frac{\partial\tau_i}{\partial z} = R_i \qquad ,\sigma>\delta \tag{2.3.6a}$$

$$\frac{\partial\tau_i}{\partial z} = R_i + \frac{\partial}{\partial z}\rho\tilde{u}_i\tilde{w} \qquad ,\sigma<\delta \tag{2.3.6b}$$

where R_i is the forcing due to inertia, curvature, Coriolis and a pressure gradient, and:

$$\frac{\partial}{\partial z}\rho\tilde{u}_i\tilde{w} = -\frac{1}{\delta}\frac{D_f k_i}{\omega} \tag{2.3.7}$$

We now make the assumption that the depth-variation of R_i can be neglected. In this case, integration of (2.3.17a) and (2.3.17b) from the surface downwards yields:

$$\tau_i = \tau_{s,i} - R_i(1-\sigma) \qquad ,\sigma>\delta \tag{2.3.8a}$$

$$\tau_i = \tau_{s,i} - R_i(1-\sigma) + \frac{D_f k_i}{\omega}\frac{\delta-\sigma}{\delta} \qquad ,\sigma>\delta \tag{2.3.8b}$$

The shear stress is related to the velocity gradients by:

$$\tau_i = \frac{\rho \nu_t}{h}\frac{\partial u_i}{\partial \sigma} \tag{2.3.9}$$

We can now obtain the velocity profile by integrating eq. (2.3.9); by integrating once more, we get the depth-mean velocity. Both integrations can be carried out analytically and yield relatively simple, logarithmic expressions. In these expressions, we have the known shear stress $\tau_{s,i}$ and bottom dissipation D_f, and the term R_i, which is dominated by the surface slope.

When we apply the expressions to obtain the longshore current profile, this surface slope is a known quantity, and the depth-mean current and the current profile are computed directly.
For the cross-shore current, the mean current is known, and R_i is obtained from the depth-averaged expression; after this the current profile can be computed directly.
Details of the computation are given in Appendix C.

Turbulence viscosity for purely slope-driven current

For purely slope-driven currents, the distribution of the eddy viscosity is parabolic, and zero at $\sigma=0$ and $\sigma=1$. This leads to $\sigma_s=1$ and $\phi_s=6$ in eq. (2.3.13).

Near the bottom, the velocity varies linearly with distance from the bed, with a gradient:

$$\frac{\partial u}{\partial \sigma} = \frac{u_*}{\kappa e \sigma_0} \tag{2.3.10}$$

For slope-driven current, we have near the bed:

$$\frac{\partial u_i}{\partial \sigma} = A\left(\frac{B_i}{\sigma_s \sigma} + \frac{B_i/\sigma_s + C_i}{\sigma_s - \sigma}\right) = \frac{h}{\rho \phi_s \overline{\nu_t}}\left(\frac{-\rho g h s_i}{\sigma_s \sigma}\right) = \frac{h}{6\rho \overline{\nu_t}}\frac{\tau_b}{e\sigma_0} \tag{2.3.11}$$

So:

$$\frac{u_*}{\kappa e \sigma_0} = \frac{h}{6\overline{\nu_t}}\frac{u_*^2}{e\sigma_0} \tag{2.3.12}$$

The depth-averaged viscosity is now expressed as:

$$\overline{\nu_{t,1}} = \frac{1}{6}\kappa h\sqrt{gh|s|} \tag{2.3.13}$$

Turbulence viscosity for wind-driven current

In the case of purely wind-driven current, it is unlikely that the viscosity goes to zero near the surface; rather, a maximum is expected there. We model this by assuming a half-parabolic distribution, with σ_s=2 and hence ϕ_s=1.5.

Near the bottom, the velocity again varies linearly with distance from the bed:

$$\frac{\partial u}{\partial \sigma} = \frac{u_*}{\kappa e \sigma_0} \tag{2.3.14}$$

For wind-driven current, we have near the bed:

$$\frac{\partial u_i}{\partial \sigma} = A\left(\frac{B_i}{\sigma_s \sigma} + \frac{B_i/\sigma_s + C_i}{\sigma_s - \sigma}\right) = \frac{h}{\rho\phi_s\overline{\nu_t}}\left(\frac{\tau_s}{\sigma_s\sigma}\right) = \frac{h}{\frac{3}{2}\rho\overline{\nu_t}}\frac{\tau_s}{2e\sigma_0} \tag{2.3.15}$$

So:

$$\frac{u_*}{\kappa e \sigma_0} = \frac{h}{3\overline{\nu_t}}\frac{u_*^2}{e\sigma_0} \tag{2.3.16}$$

The depth-averaged viscosity is now expressed as:

$$\overline{\nu_{t,2}} = \frac{1}{3}\kappa h\sqrt{\frac{|\tau_s|}{\rho}} \tag{2.3.17}$$

Turbulence viscosity generated by wave breaking

The depth-averaged turbulence viscosity due to wave breaking is modelled according to Battjes (1975) as:

$$\overline{\nu_{t,3}} = \alpha_w\left(\frac{D}{\rho}\right)^{1/3} L \tag{2.3.18}$$

where α_w is a coefficient and L is a typical length scale. Validation studies (LIP Delta Flume Experiment, LIP Shear Wave Experiment indicate that choosing $L=H_{rms}$ in combination with α_w in the range of 0.05-0.10 leads to optimum results.

The distribution over the depth of the breaking-induced turbulence is assumed to be similar to that induced by wind stress.

Combination of turbulence viscosity from different sources

In the case that we have turbulence generated by different sources, a zero-equation turbulence model cannot be derived rigorously. We therefore have to choose a reasonable approximation, which meets a number of constraints:

- the combined viscosity profile must reduce to all of the above mentioned limit cases;
- given that the length scales must be similar for the processes mentioned, it seems reasonable to add turbulence energy from different sources. For the viscosity, since $\nu_t = \sqrt{\mu/l}$, we must therefore take the rms of the different viscosity components;
- to ensure that the equations can be solved analytically, the combined viscosity profile must be of the form described by eq. (2.3.1).

The second and third constraint cannot be met exactly at the same time. However, a good approximation is

$$\overline{\nu_t} = \sqrt{\overline{\nu_t}^2_{current} + \overline{\nu_t}^2_{wind} + \overline{\nu_t}^2_{breaking}} \tag{2.3.19}$$

$$\nu_{t,surface} = \frac{3}{2}\sqrt{\overline{\nu_t}^2_{wind} + \overline{\nu_t}^2_{breaking}} \tag{2.3.20}$$

The parameters ϕ_s and σ_s can now be determined from:

$$\sigma_s = \frac{\overline{\nu_t} - \frac{1}{3}\nu_{t,surface}}{\overline{\nu_t} - \frac{1}{2}\nu_{t,surface}} \tag{2.3.21}$$

$$\phi_s = \frac{1}{\frac{1}{2}\sigma_s - \frac{1}{3}} \tag{2.3.22}$$

Increased turbulence in wave boundary layer

$$\overline{\nu_{tb}} = \frac{1}{2}\kappa h u_{*w}\delta \tag{2.3.23}$$

$$u_{*w} = \sqrt{\frac{f_w}{2}}\hat{u}_{orb} \tag{2.3.24}$$

2.4 Near-bed orbital velocity

The model of the time-variation of the near-bed velocity (orbital motion) due to non-linear short waves and long waves related to wave groups is based on the concept described in Roelvink and Stive (1989). In short, this model consisted of two parts:

- a contribution due to wave asymmetry which is computed using Rienecker and Fenton's (1981) method for monochromatic waves, where the mean wave energy and peak period are used as input for the case of random waves; in case broken waves are present, the asymmetry is reduced as function of the fraction of breaking waves.
- a contribution due to bound long waves based on Sand (1982), and an empirical relationship for the phase of the bound wave relative to the short wave envelope.

The sediment transport model in the previous version of UNIBEST required only velocity moments, rather than a complete time-series. Therefore it was possible to compute the two contributions to the velocity moments separately and add the result.

In the present transport model, a complete representative time-series of the near-bed velocity is required. The model has now been adapted to produce such a time-series, which has the same characteristics of asymmetry, long waves and amplitude modulation. The shortest time-series which can exhibit all of these features has a length of one short wave group, which is m waves long.

The method followed is outlined below:

First, a time series for regular waves is generated based on the Rienecker and Fenton model:

$$U_1(t) = (1-Q_b)\sum_{j=1}^{n}\cos(j\,\omega\,t) + Q_b\sum_{j=1}^{n}\sin(j\,\omega\,t) \qquad (2.4.1)$$

Second, this time series is modulated, according to:

$$U_2(t) = (1-Q_b)\sum_{j=1}^{n}\cos(j\,\omega\,t)\,\epsilon^j + Q_b\sum_{j=1}^{n}\sin(j\,\omega\,t)\,\epsilon^j \qquad (2.4.2)$$

where:

$$\epsilon = \frac{1}{2}(1+\cos(\Delta\omega t)) \qquad (2.4.3)$$

and

$$\Delta\omega = \omega/m \qquad (2.4.4)$$

The notation ϵ^j here means "ϵ to the power j".

The magnitude of U_2 is then corrected to U_2' in such a way, that the third moment of U_2' is equal to the third moment of U_1:

$$U_2' = \left(\frac{\frac{1}{T}\int_0^T U_1^3\,dt}{\frac{1}{mT}\int_0^{mT} U_2^3\,dt} \right)^{1/3} U_2 \qquad (2.4.5)$$

In case of a random wave field the grouping of the short waves will generate bound long waves. The long wave velocity u3 is computed according to Roelvink and Stive (1989) where they assume that the wave-group related features of a random wave field may be represented by a bichromatic wave train and accompanying bound long wave. The amplitude of the bound long wave is computed according to Sand (1982):

$$\xi_a = -G_{mn}\frac{a_n a_m}{h} \qquad (2.4.6)$$

where the short wave amplitudes are given by

$$a_n^2 = a_m^2 = \frac{1}{8}H_{rms}^2 - \frac{1}{2}\xi_a^2 \qquad (2.4.7)$$

The velocity due to the long wave component is then given by

$$U_3 = \hat{u}_l \cos(\omega_l t) \qquad (2.4.8)$$

where

$$u_l = \xi_a \frac{\sqrt{gh}}{h} \qquad (2.4.9)$$

and

$$\omega_l = \frac{\omega}{5} \qquad (2.4.10)$$

The total orbital velocity U_4 is computed simply by adding U_2' and U_3.

2.5 Bed-load transport

A brief summary is given here; a more extended description is given by Van Rijn et al., 1995. For the *non-dimensional transport rate* the following parameters are distinguished.

$$\Phi_{bw} = q_b/(w_s d_{50}) \qquad (2.5.1)$$

i.e. the ratio of bed-load transport rate q_b and a settling flux parameter $w_s d_{50}$

$$\Phi_{bd} = q_b/(\Delta g d_{50}^3)^{0.5} \qquad (2.5.2)$$

i.e. the ratio of bed-load transport rate q_b and the square-root of a parameter representing the specific under-water weight of sand grains.

For the *non-dimensional sediment forcing* the following parameters are distinguished.

$$\theta = \tau_b/((\rho_s-\rho)gd_{50}) \tag{2.5.3}$$

i.e. the Shields parameter, representing the ratio of the flow drag-force on the grains and the under-water weight of grains.

$$u_*/w_s \tag{2.5.4}$$

i.e. the ratio of friction velocity u_* and settling velocity w_s of sand.

$$u_b/w_s \tag{2.5.5}$$

i.e. ratio of horizontal near-bed velocity u_b and w_s.

Moreover, the following non-dimensional parameters will be used (see Van Rijn, 1993):

$$\theta_c = F(D_*) \tag{2.5.6}$$

i.e. the critical Shields parameter, representing the threshold of motion of sand grains, and as non-dimensional grain size:

$$D_* = d_{50}(g\Delta/\nu^2)^{1/3} \tag{2.5.7}$$

Herein:

q_b = bed-load transport rate in volume per unit time and width
d_{50} = median grain diameter
w_s = settling velocity
Δ = relative density = $(\rho_s - \rho)/\rho$
ρ_s = density of sand
ρ = density of water
g = gravity acceleration
τ_b = bed-shear stress
ν = kinematic viscosity of water
u_* = friction velocity ($= \sqrt{\tau_b/\rho}$)
u_b = horizontal near-bed velocity

In the present study a quadratic friction law is applied, using intra-wave near-bed velocities of the combined wave-current motion and a weighed friction factor f'_{cw}. For the generalized 2DH situation (x - y):

$$\begin{aligned} q_{bx} &= |\, q_b \,|\, u_{bx}/|\, u_b \,| \\ q_{by} &= |\, q_b \,|\, u_{by}/|\, u_b \,| \end{aligned} \tag{2.5.8}$$

in which u_b and q_b are respectively the time-dependent (intra-wave) near-bottom horizontal velocity vector (at $z = \delta$) and the bed-load transport vector of the combined wave-current motion.

The instantaneous bed-load transport vector ϕ_{bd} is computed with:

$$\Phi_{bd}(t) = q_b(t)/(\Delta g d_{50}^3)^{0.5} = 9.1 \{ | \theta'(t) | - \theta_c \}^{1.78} \theta'(t)/ | \theta'(t) | \qquad (2.5.9)$$

using:

$$\theta'(t) = \tfrac{1}{2} \rho f'_{cw} | u_b(t) | u_b(t)/((\rho_s-\rho) g d_{50}) \qquad (2.5.10)$$

where $\theta'(t)$ is the instantaneous dimensionless shear stress due to currents and waves.

Following van Rijn (1993) the wave-current friction factor f'_{cw} is computed from the (skin) friction factors for 'waves alone' and 'steady currents', weighted linearly with the relative strength of the near-bed net current and oscillatory velocity amplitude as described below.

In the case of combined waves and currents an approach as suggested by Grant and Madsen (1979) is used by assuming that the bed shear stress can be expressed as a quadratic function of the combined wave/current velocity at some height z above the bed (above the wave boundary layer):

$$\tau_b(t) = \tfrac{1}{2} \rho f'_c | u_b(t) | u_b(t) \qquad (2.5.11)$$

In principle the problem is 2DH now since waves and currents may interact under an arbitrary angle. The bed-shear stress τ_b and near-bed velocity u_b are vectors in the same direction with varying magnitudes and varying directions during the wave cycle.

Research is still carried out aiming at a the development of simple formulations for the time-dependent bed shear stress under combined currents and waves (see Soulsby et al, 1993; Ockenden and Soulsby, 1994). In the present study the above mentioned quadratic friction law is used together with a weighted friction coefficient for currents and waves. Following van Rijn (1993):

$$f'_{cw} = \alpha f'_c + (1-\alpha) f'_w \qquad (2.5.12)$$

with:

$$\alpha = <u_b> / (<u_b> + \hat{U}) \qquad (2.5.13)$$

in which:

$<u_b>$ = time-averaged or mean current near-bed velocity (at level z)
$\hat{U}$ = velocity amplitude of the wave-induced oscillatory flow near the bed (without mean current)

For the computation of the roughness height k_s in the sheet flow regime ($\theta' > 1$) a mean bed-shear stress (or Shields parameter) is necessary, which itself is dependent of k_s .

An iterative procedure is followed in which a mean bed-shear stress is first estimated with input of the grain roughness $k_s = 3d_{90}$ using the following expression:

$$< | \tau_b | > = \tfrac{1}{4} \rho f'_w \hat{U}^2 + \tfrac{1}{2} \rho f'_c <u_b>^2 \qquad (2.5.14)$$

With this bed-shear stress a new estimate of k_s is obtained using $k_s = 3\theta' d_{90}$ and the computation is repeated until the solution converges and changes less than 1% during the last iteration.

The net wave-averaged bed-load transport rate is obtained by averaging of the time-dependent transport vector $q_b(t) = (q_{bx}, q_{by})$ over the duration of the imposed near bottom velocity time series.

2.6 Suspended transport

The suspended sediment transport rate (q_s) can be computed from the vertical distribution of fluid velocities and sediment concentrations, as follows:

$$q_s = \int_a^{h+\eta} VC \, dz \qquad (2.6.1)$$

in which:

- V = local instantaneous fluid velocity at height z above bed (m/s)
- C = local instantaneous sediment concentration at height z above bed (kg/m^3)
- h = water depth (to mean surface level), (m)
- η = water surface elevation (m)
- a = thickness of bed-load layer (m)

Defining: $V = v + \tilde{v}$ and $C = c + \tilde{c}$ (2.6.2)

in which:

- v = time and space-averaged fluid velocity at height z (m/s)
- c = time and space-averaged concentration at height z (m/s)
- $\tilde{v}$ = oscillating fluid component (including turbulent component), (m/s)
- $\tilde{c}$ = oscillating concentration component (including turbulent component), (m/s)

Substituting Eq. (2.6.2) in Eq. (2.6.1) and averaging over time and space yields:

$$\bar{q}_s = \int_a^h vc \, dz + \int_o^h \overline{\tilde{v}\tilde{c}} \, dz = \bar{q}_{s,c} + \bar{q}_{s,w} \qquad (2.6.3)$$

in which:

$$\bar{q}_{s,c} = \int_a^h vc \, dz = \text{time-averaged current-related sediment transport rate (kg/sm)}$$

$$\bar{q}_{s,w} = \int_a^h \overline{\tilde{v}\tilde{c}} \, dz = \text{time-averaged wave-related sediment transport rate (kg/sm)}$$

The current-related suspended sediment transport is defined as the transport of sediment particles by the time-averaged (mean) current velocities (longshore currents, rip currents, undertow currents). The current velocities and the sediment concentrations are affected by the wave motion. It is known that the wave motion reduces the current velocities near the bed, but the wave motion strongly increases the near-bed concentrations due to its stirring action. The wave-related suspended sediment transport is defined as the transport of sediment particles by the oscillating fluid components (cross-shore orbital motion).

In this Section the attention is focused on the current-related transport rate.

Time averaged concentration profile

Usually, the convection-diffusion equation is applied to compute the equilibrium concentration profile in steady flow. This equation reads as:

$$w_{s,m} + \epsilon_{s,cw} \frac{dc}{dz} = 0 \qquad (2.6.4)$$

in which:

$w_{s,m}$ = fall velocity of suspended sediment in a fluid-sediment mixture (m/s)
$\epsilon_{s,cw}$ = sediment mixing coefficient for combined current and waves (m^2/s)
c = time-averaged concentration at height z above the bed (kg/m^3)

Here, it is assumed that Eq. (2.6.4) is also valid for wave-related mixing.

Sediment mixing coefficient

For combined current and wave conditions the sediment mixing coefficient is modeled as:

$$\epsilon_{s,cw} = \left[(\epsilon_{s,w})^2 + (\epsilon_{s,c})^2\right]^{0.5} \qquad (2.6.5)$$

in which:

$\epsilon_{s,w}$ = wave-related mixing coefficient (m^2/s)
$\epsilon_{s,c}$ = current-related mixing coefficient (m^2/s)

First, the wave-related mixing is discussed.

Measurements in wave flumes show the presence of suspended sediment particles from the bed up to the water surface (Van Rijn, 1993). The largest concentrations are found close to the bed where the diffusivity is large due to ripple-generated eddies. Further away from the bed the sediment concentrations decrease rapidly because the eddies dissolve rather rapidly travelling upwards.

Various researchers have tried to model the suspension process by introducing an effective wave-related sediment mixing coefficient (Van Rijn, 1993).

Based on analysis of measured concentration profiles, the following characteristics were observed (Van Rijn, 1993);

- approximately constant mixing coefficient $\epsilon_{s,w,bed}$ in a layer ($z \leq \delta_s$) near the bed,
- approximately constant mixing coefficient $\epsilon_{s,w,max}$ in the upper half ($z \geq 0.5$ h) of the water depth,
- approximately linear variation of the mixing coefficient for $\delta_s < z < 0.5$ h.

The mathematical formulation reads as:

$$z \leq \delta_s \qquad \epsilon_{s,w} = \epsilon_{s,w,bed} \tag{2.6.5a}$$

$$z \geq 0.5\ h \qquad \epsilon_{s,w} = \epsilon_{s,w,max} \tag{2.6.5b}$$

$$\delta_s < z < 0.5\ h \qquad \epsilon_{s,w} = \epsilon_{s,w,bed} + [\epsilon_{s,w,max} - \epsilon_{s,w,bed}] \left[\frac{z-\delta_s}{0.5h-\delta_s}\right] \tag{2.6.5c}$$

Equation (2.6.4) is fully defined when the following three parameters are known:

1. Thickness of near-bed sediment mixing layer (δ_s)
   Based on analysis of concentration profiles measured in non-breaking waves, it was found that:

   $\delta_s = 3\ \Delta_r$ (ripple height)
   $\delta_s = 3\ \delta_w$ (sheet flow regime)

   in which:

   Δ_r = ripple height (m)
   $\delta_w = 0.072\ \hat{A}_\delta\ (\hat{A}_\delta/k_{s,w})^{-0.25}$ = wave boundary layer thickness (m)
   δ_s = thickness of near-bed sediment mixing layer (m)
   $k_{s,w}$ = wave-related bed roughness height (m)
   $\hat{A}_\delta$ = peak value of near-bed orbital excursion (m)

2. Mixing coefficient in near-bed layer ($\epsilon_{s,w,bed}$)

   This parameter was found to be:

$$\epsilon_{s,w,bed} = \alpha_b\ \hat{U}_\delta\ \delta_s \tag{2.6.6}$$

   in which:

   $\hat{U}_\delta$ = peak value of near-bed orbital velocity (based on significant wave height) (m/s)
   $\alpha_b = 0.004\ D_*$ = empirical coefficient (-)
   $D_* = d_{50}\ [(\rho_s - \rho)g/(\rho\nu^2)]^{1/3}$ = particle size parameter (m)

3. Mixing coefficient in upper layer ($\epsilon_{s,w,max}$)

This parameter was found to be:

$$\epsilon_{s,w,max} = 0.035 \frac{H_s h}{T_p} \tag{2.6.7}$$

in which:

H_s = significant wave height (m)
T_p = peak period of spectrum (s)
h = water depth (m)

Current-related mixing

Second, the current-related mixing coefficient ($\epsilon_{s,c}$) is presented, which reads as:

$$\epsilon_{s,c} = \kappa \beta u_{*,c} z(1-z/h) \qquad \text{for } z < 0.5\ h$$
$$\epsilon_{s,c} = 0.25 \beta \kappa u_{*,c} h \qquad \text{for } z \geq 0.5\ h \tag{2.6.8}$$

in which:

$u_{*,c}$ = $(g^{0.5} \bar{v})/C$ = bed-shear velocity (m/s)
C = 18 log $(12h/k_{s,c})$ = Chézy coefficient ($m^{0.5}/s$)
$\bar{v}$ = depth-averaged velocity vector (m/s)
$k_{s,c}$ = current-related bed-roughness height (m)
h = water depth (m)
κ = constant of Von Karman (= 0.4)
ß = coefficient (= 1)

Reference concentration near the bed

The reference concentration is given by:

$$c_a = 0.015 \frac{d_{50}}{a} \frac{T^{1.5}}{D_*^{0.3}} \tag{2.6.9}$$

in which:

D_* = dimensionless particle parameter (-)
T = dimensionless bed-shear stress parameter (-)
a = thickness of bed-load layer or reference level (m)

The T-parameter is, as follows:

$$T = [\tau'_{b,cw} - \tau'_{b,cr}]/\tau_{b,cr} \qquad (2.6.10)$$

in which:

$\tau'_{b,cw}$ = time-averaged effective bed-shear stress (N/m^2)
$\tau'_{b,cr}$ = time-averaged critical bed-shear stress according to Shields (N/m^2)

The magnitude of the time-averaged bed-shear stress, which is independent of the angle between the wave- and current direction is given by (Van Rijn, 1993):

$$\tau'_{b,cw} = \tau'_{b,c} + \tau'_{b,w} \qquad (2.6.11)$$

in which:

$\tau'_{b,c} = \mu_c \alpha_{cw} \tau_{b,c}$ = effective current-related bed-shear stress (N/m^2)
$\tau'_{b,w} = \mu_w \tau_{b,w}$ = effective wave-related bed-shear stress (N/m^2)
$\tau_{b,c} = \frac{1}{8} \rho f_c (\bar{v})^2$ = current-related bed-shear stress (N/m^2)
$\tau_{b,w} = \frac{1}{4} \rho f_w (\hat{U}_\delta)^2$ = wave-related bed-shear stress (N/m^2)
$f_c = 0.24 [\log (12h/k_{s,c})]^{-2}$ = current-related friction factor (-)
$f'_c = 0.24 [\log (12h/3d_{90})]^{-2}$ = grain friction factor (-)
$f_w = \exp[-6 + 5.2(\hat{A}_\delta/k_{s,w})^{-0.19}]$ = wave-related friction factor (-)
$\bar{v}$ = depth-averaged current-velocity vector (m/s)
$\hat{U}_\delta$ = peak value of near-bed orbital velocity (m/s)
$\hat{A}_\delta$ = peak value of near-bed orbital excursion (m)
h = water depth (m)
$k_{s,c}$ = current-related bed-roughness (m)
$k_{s,w}$ = wave-related bed-roughness (m)
$\mu_c = f'_c/f_c$ = current-related efficiency factor (-)
$\mu_w = 0.6/D_*$ = wave-related efficiency factor (-)
α_{cw} = correction factor related wave-current interaction (-)
ρ = fluid density (kg/m^3)
ρ_s = sediment density (kg/m^3)

The suspended load transport is given by:

$$q_{s,c} = \int_a^h vc \, dz \qquad (2.6.12)$$

3 Running the model

3.1 Introduction

In the input parameters required to run the UNIBEST program are treated using a demo input file (which is also included as an appendix). The input-file is treated line by line, where lines preceded by an asterix are comment lines (which have to be present) in the input file, followed by a line which contains the input values. Note that the input file is very similar to the input file used in the previous version of UNIBEST-TC. A more detailed explanation of many of the input parameters is given in the UNIBEST-TC manual.
At this moment it is not possible to use the UNIBEST-TC pre-processor to create input-files. Instead, already existing input files should be edited to create new input files.

3.2 Description of input file

```
RUNIDENTIFICATIE          (lees in uni_tc.for)        (file demox.da
    208
```

The run identification has to be three digit number, therefore ranging from 000 to 999. This number is used to denote the output files generated by the program, showing which output files belong to which input file.

```
GRID
     X_BEGIN NDX
     0.0   3
     NUMBER  DX        (total number < 119)
     25      4.
     10      2.
     80      1.
```

Definition of the numerical grid, starting at X_BEGIN. Next the number of lines used to define the grid have to be given, in this case three, with 25 meshes of 4 metres, 10 of 2 metres and 80 of 1 metre.

```
RUNPARAMETERS              (lees in inpx.dat)
        DT(day) NT   JCLOSE(-1,1,2) USTRA(m3/h)  JFR  IBOD  TDR
        1.0      0   -1              0.0         1    0     40.
        DUM1   DUM2   DUM3   DUM4   DUM5   DUM6   DUM7   FACVISC
        1.     1.     1.     1.     1.     1.     1.     0.1
```

DT : time step in days
NT : number of time steps
JCLOSE : defines the shoreward boundary condition
-1 : current transport
1 : no transport
2 : user defined transport (USTRA)
JFR : frequency of output to *.daf file (JFR = 1 means every time step)

IBOD :

0 : bottom changes not computed

1 : compute bottom changes

TDR : relative wave-period, detremines the minimum water depth up to which the computation is performed (40 for prototype conditions)

FACVISC : viscosity coefficient velocity profile

```
* COEFFICIENTS WAVES  AND FLOW
*        GAMMA   ALFAC   FWEE    RKVAL   DIEPV   REMLAAG  BETD
         0.0     1.0     0.01     0.01    5.0     0.10      .1
```

GAMMA : wave breaking parameter, set to 0.0 for default value according to Stive&Battjes

ALFAC : wave breaking parameter

FWEE : friction factor for wave dissipation due to bottom friction

RKVAL : friction factor for mean current computation

DIEPV : reference depth for tidal velocity

REMLAAG : layer in which the sediment transport is reduced to zero in case of a fixed bed

BETD : factor used in roller formulation, expressing the steepness of the wave front

```
* COEFFICIENTS VELOCITIES AND TRANSPORTS
*     D50       D90     DSS     RC      RW      PHILAT  DRHODX  DRHODY
      .19e-3    .3e-3   .16e-3  .01     .0       52.0    0.0     0.0
```

D50 : D50 grain diameter (m)

D90 : D90 grain diameter (m)

DSS : D50 grain diameter of suspended sediment (m)

RC : current related roughness for sediment transport computation (m)

RW : wave related roughness for sediment transport computation (m)

PHILAT : latitude on earth

DRHODX : density gradient in x-direction $kg/m^{3}/m$

DRHODY : density gradient in y-direction $kg/m^{3}/m$

```
*        TEMP    SALIN   C_R
         10.0     0.      .25
```

TEMP : temperature of water

SALIN : salinity in 0/00

C_R : correlation coefficient between wave envelope and bound long waves

```
* RANDVOORWAARDEN          (9 rvw-functies in deze volgorde)
*         FUNCTION     CODE     VALUE    COLUMN   FILE
         'HO     '      1        4.0667   0        ' '
         'V_TIDE'       1        0.0      0        ' '
         'A_WAVE'       1        0.0      0        ' '
         'HRMS   '      1        .9579    0        ' '
         'T      '      1        5.0      0        ' '
         'Z      '      2        0.0      1        '%1b08mc.dat'
         'Z_FIX  '      1       -30.0     0        ' '
         'V_WIND'       1        0.0      0        ' '
         'A_WIND'       1        20.0     0        ' '
```

There is an option to introduce a file which contains the values for the boundary conditions by setting CODE to 2. This means a filename has to be specified which contains the selected variable. This can either a bottom profile in case of Z and Z-fix or a time series in case of any of the other variables If CODE is set at 1, a value for the selected variable has to be given in the column VALUE.

FUNCTION	:	variable
CODE	:	
1	:	means constant value
2	:	means read value from FILE
VALUE	:	value of variable
COLUMN	:	number of column in FILE with values for variable
FILE	:	filename of file, note that there is a standard file format (example included in Appendix B)
H0	:	water level (m)
V_TIDE	:	tidal velocity at reference depth (m/s)
A_WAVE	:	wave direction w.r.t coast normal (deg)
HRMS	:	root mean square wave height (m)
T	:	peak wave period (s)
Z	:	bottom level (m)
Z	:	fixed bottom level (m)
V_WIND	:	wind velocity (m/s)
A_WIND	:	wind direction (deg)

```
* BASICFUNCTIONS                    (lees in outfil.for)
*        X-POINTS FOR TIMEFUNCTIONS (COLUMNS ON UTC###.HIS)
        2
```

Define number of points along the profile where output of time series is required.

```
*        NR    X-POINT
         1     160.000
         2     170.000
```

NR : location number
X : position w.r.t. X_BEGIN

```
*NUMBER OF ACTUAL TIMEFUNCTIONS
        2
*        FUNC  1  2                    (FUNC 1:29)
         1     1  1
         2     0  1
```

There are 29 functions for which output can be generated (see appendix) First the number of function is defined, next their identification number (FUNC) has to be given. By setting the value in the second column to 1 a time series for that specific variable (defined by FUNC) is generated at location 1 (defined previously). If set to zero, no time series will be generated at location 1. So in this case timeseries for FUNC = 1 (bottom level) is generated at locations 1 and 2. For FUNC = 2 (wave height) timeseries are generated at location 2 only. Output is written to a *.his file.

```
*        T-POINTS FOR PLACE-FUNCTIONS (BLOCKS ON UTC###.MP@)
         1
*        NR   T_POINT
         1      1.0
NUMBER OF ACTUAL PLACE FUNCTIONS
        10
        FUNC      @  1  2  3  4  5  6       (FUNC 1:29)
        1         1  1
        2         1  1
        3         1  1
        15        1  1
        16        1  1
        17        1  1
        18        1  1
        22        1  1
        24        1  1
        26        1  1
```

Instead of generating time series, it is also possible to generate files which give the cross-shore distribution of a variable (again defined by FUNC). The concept is exactly the same. Output is written to a *.mp1 file.

```
*VOLUMINA
        2
*        X1             X2              H
        88.000000      138.000000      -5.000000
        138.000000     188.000000      -3.000000
```

Option to compute the changes in volume for user defined control-areas.

X1 : starting point (m)
X2 : end-point (m)
H : reference level (m)

```
* VERT.FUNCTIONS
       9
*       X_POINT       T_POINT      F-TYPE (1=Z, 2=T, 3=BOTH)
         65.0         1.0          1
        100.0         1.0          1
        115.0         1.0          1
        130.0         1.0          1
        138.0         1.0          1
        142.0         1.0          1
        152.0         1.0          1
        160.0         1.0          1
        170.0         1.0          1
```

A new feature is the possibility to store the vertical distribution of the return flow and sediment concentration in a file, the time series of the near-bed orbital velocityp or both. This is done by defining the number of locations and at what time step which output is to be generated. Output is written to a *.ver file.

X_POINT : output location
T_POINT : time step
F-TYPE :
1 : vertical distribution
2 : time series
3 : both

3.3 Computation

One the input file is created the model computation is started by typing:

unibest_tc.exe

followed by a return. Next the program asks for the name of the input file, after this is given the computation proceeds.

3.4 Post processing

All post-processing features remain the same as in the previous version. Therefore the post-processing program viz_tc can still be used to examine the computational results stored in the *.daf file. Otherwise defined output, ie time series (*.his), cross-shore distribution of variables (*.mp1), vertical distributions (*.ver), etc are written to files in ascii using a standard format which gives the possibility to use other post-processing software (eg tekal).

4 Model performance

To check whether the upgraded formulations have been implemented correctly a number of tests have been performed prior to the validation process, including comparisons of results with the upgraded and 'old' numerical model. Some typical results of comparisons with data available from the Delta-flume experiment (part of the validation study: H2130) are shown in Figures 4.1 to 4.4.

Graph A in Figure 4.1 shows the comparison of the computational results obtained for wave height with measurements. It shows that the wave height is predicted accurately throughout the flume, except for the small discrepancy in the trough. This result is typical for most of the LIP11D-data set. The overestimation of the wave height in the trough indicates that waves breaking on the bar do not reform as quickly as computed by the model (i.e. continued dissipation).

Graph B shows the lag-effect in the dissipation due to the roller. As the waves start breaking there is a decrease in wave energy denoted by D_w, computed with the BJ-model, and a corresponding built-up of the roller-energy. Next this roller energy is dissipated, denoted by *Diss*, due to friction between the propagating roller and the underlying water mass. The effect of the roller on the mass flux is shown in graph A, where there is an increase in the flux on top of the bar due to increased wave breaking and thus build up of the roller.

The comparison between computed and measured set-up values is shown in graph D of Figure 1. The measured set-up values have been obtained from pressure sensors. It shows that there is a good qualitative and quantitative agreement, again with maximum differences occurring in the trough.

To validate the asymmetry of the waves the third order velocity moment:

$$guss = <u_s(t)|u_s(t)|^2> \tag{4.1}$$

is used, where the short wave velocity, $u_s(t)$, is computed with the stream function theory of Rienecker and Fenton (eq. 2.4.5). A comparison of computational results with measurements is shown graph H of Figure 4.2. Note that the asymmetry is weighted with the fraction of breaking waves. If all waves are breaking the asymmetry is assumed to be zero. On top of the bar (x = 138 m) and at the step (x = 160 m) the fraction of breaking waves is relatively high, and the computed and measured velocity moments correspond well. In the trough, the wave asymmetry is overestimated due to an underestimation of the fraction of breaking waves.

In this case the bound long wave compares favourably with the measurements as shown in graph F of Figure 4.2, where another a third order velocity moment:

$$gusl = <3u_f(t)|u_s(t)|^2> \tag{4.2}$$

was used.

The results for the return flow at 10 cm above the bed-level and the vertical distribution are shown in graph G of Figure 4.2 and Figure 4.3 respectively. Offshore of the bar the return flow is being overestimated followed by an underestimation of the return flow in the trough, indicating a stronger lag-effect than what follows from the computations. Near the shore the return flow is again overestimated.

The comparison of the computed and measured time-averaged vertical distribution of the sediment concentration is shown in Figure 4.4. This shows that offshore the reference concentration is too high, resulting in an overprediction of the concentration in the vertical. As wave breaking intensifies closer to the shore line, the results improve considerably.

The resulting bed-and suspended load sediment transports are shown in graph J of Figure 4.2. For the bed-load transport we can see that offshore the wave-asymmetry is dominant over the return flow and bound long wave contributions. Further inshore and on top of the bar, the return flow prevails, resulting in an offshore directed bed-load transport. The suspended sediment transport is always directed offshore, in correspondence with the direction of the return flow.

5 Yearly averaged sediment transport rates

To compute the yearly averaged sediment transports a procedure similar to the one used for the JGZ-model (H1887) is used.
The wave propagation model computes the wave energy decay along a wave ray based on shoaling, refraction and energy dissipation by bottom friction and wave breaking.
The near-bed instantaneous velocities are computed as time series representing irregular wave groups (including wave asymmetry and bound long wave effects).

The vertical flow structure model computes the vertical distribution of the horizontal flow velocities for a given depth-averaged velocity vector (including wind-driven currents), wave height and period. The effect of wave breaking resulting in a longshore current and a cross-shore return current (undertow) is also taken into account.

The sand transport model computes the magnitude and direction of the bed load and suspended load transport. The bed-load transport is computed by using the instantaneous near-bed velocities which are transferred to bed-shear stresses (within the wave period). Input are the time series velocity data and the time-averaged velocity data computed by the wave model and the vertical structure model. The suspended load transport is computed from the time-averaged velocity and concentration profile.

The sediment transport rates are computed for the schematised yearly wave climate and corresponding current conditions. Tidal averaging is applied to obtain the tide-averaged transport rate for each wave direction and wave height class. The tide-averaged transport rate is multiplied by the percentage of occurrence of each specific wave condition, resulting in the weighted transport rate. Adding all individual weighted values, yields the yearly-averaged sediment transport rate.

References

Battjes, J.A., and J.P.F.M. Janssen (1978). Energy loss and set-up due to breaking in random waves. Proc. 16th Int. Conf. on Coastal Eng., ASCE, pp. 569-587.

Madsen, O.S. and W.D. Grant, 1976. Sediment transport in the coastal environment, MIT Ralph M. Parsons Lab., Rep. 209.

Nairm, R.B.J.A., (Dano) Roelvink and H.N. Southgate, 1990. Transition zone width and implications for modelling surfzone hydrodynamics. Proceedings of the Int. Conf. Vol. 2, pp. 68-82, 22 Coastal Engineering Conference, Delft, The Netherlands.

Ockenden , M. and R.L. Soulsby, 1994. Sediment transport by currents plus irregular waves, Hydraulics Research Wallingford, Report SR 376, February.

Reinecker, M.M. and J.D. Fenton (1981). A Fourier approximation method for steady water waves. J. Fluid Mech., vol. 104, pp. 119-137.

Roelvink J.A. and M.J.F. Stive, 1989. Bar-generating cross-shore flow mechanisms on a beach. J.G.R., Vol. 94, no. C4, pp. 4785-4800.

Rijn, L.C. van, 1993. Principles of sediment transport in rivers, estuaries and coastal seas. Aqua Publ. (The Netherlands).

Rijn, L.C. van et al., 1995. Yearly-averaged sand transport at the 20 m and 8 m NAP depth contours of the JARKUS-profiles 14, 40, 76 and 103, Report H18987, DELFT HYDRAULICS.

Sand, S.E., 1982. Long wave problems in laboratory models. J. Waterw. Port Coastal Ocean Div. Am. Soc. Civ. Eng., 108, pp. 492-503.

Soulsby, R.L., L. Hamm, G. Klopman, D. Myrhaug, R.R. Simons and G.P. Thomas, 1993. Wave-current interaction within and outside the bottom boundar layer, Coastal Engineering, 21, pp. 41-69.

Vriend, H.J. de and Stive, M.J.F., 1987. Quasi-3D modelling of nearshore currents. In: P.P.G. Dyke (ed), JONSMOD'86, Coastal Eng. 11, pp. 565-601.

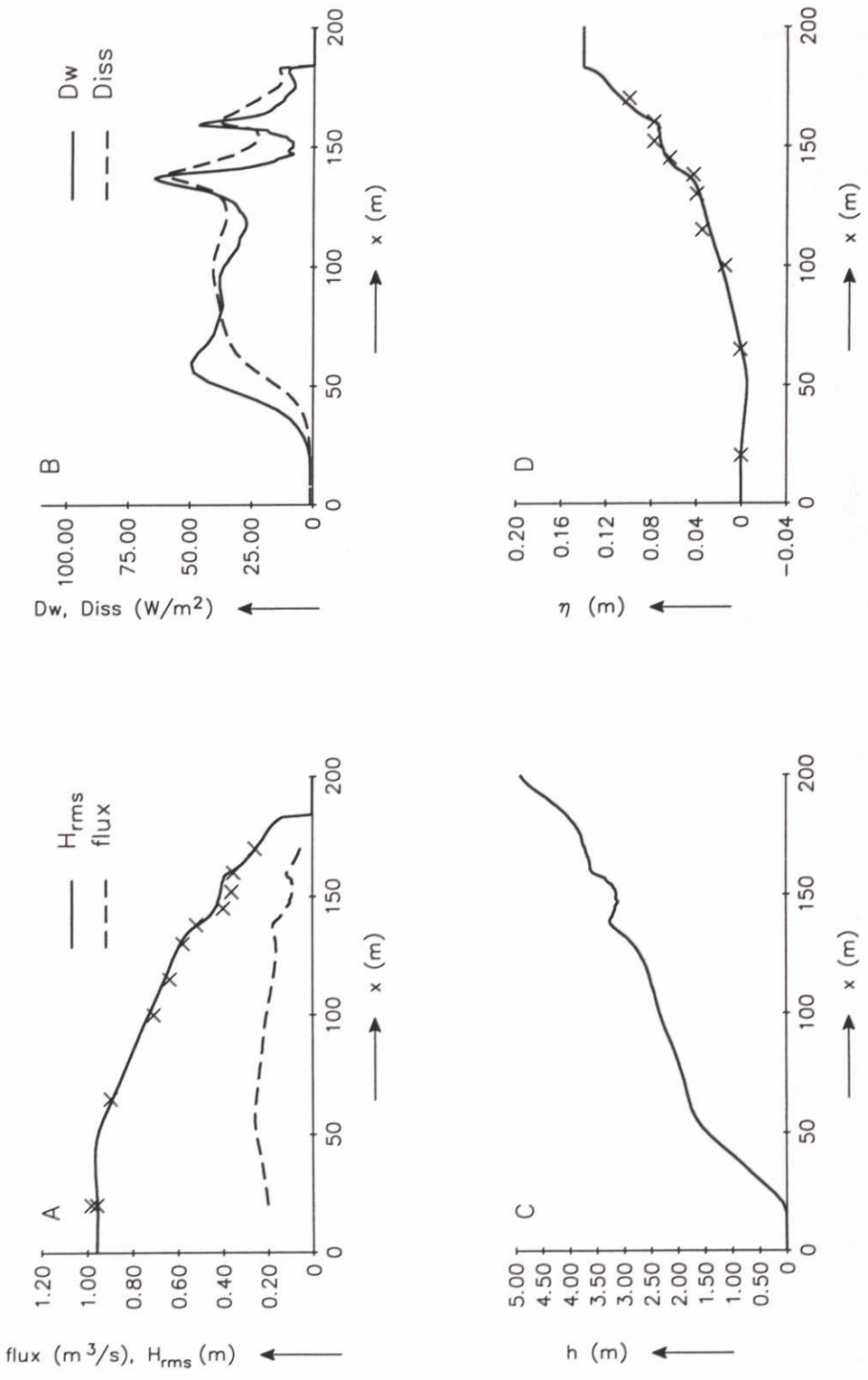

PERFORMANCE TRST UNIBEST–TC	TEST 1B	
DELFT HYDRAULICS	H 2129	FIG. 4.1

PERFORMANCE TEST UNIBEST–TC	TEST 1B	
DELFT HYDRAULICS	H 2129	FIG. 4.2

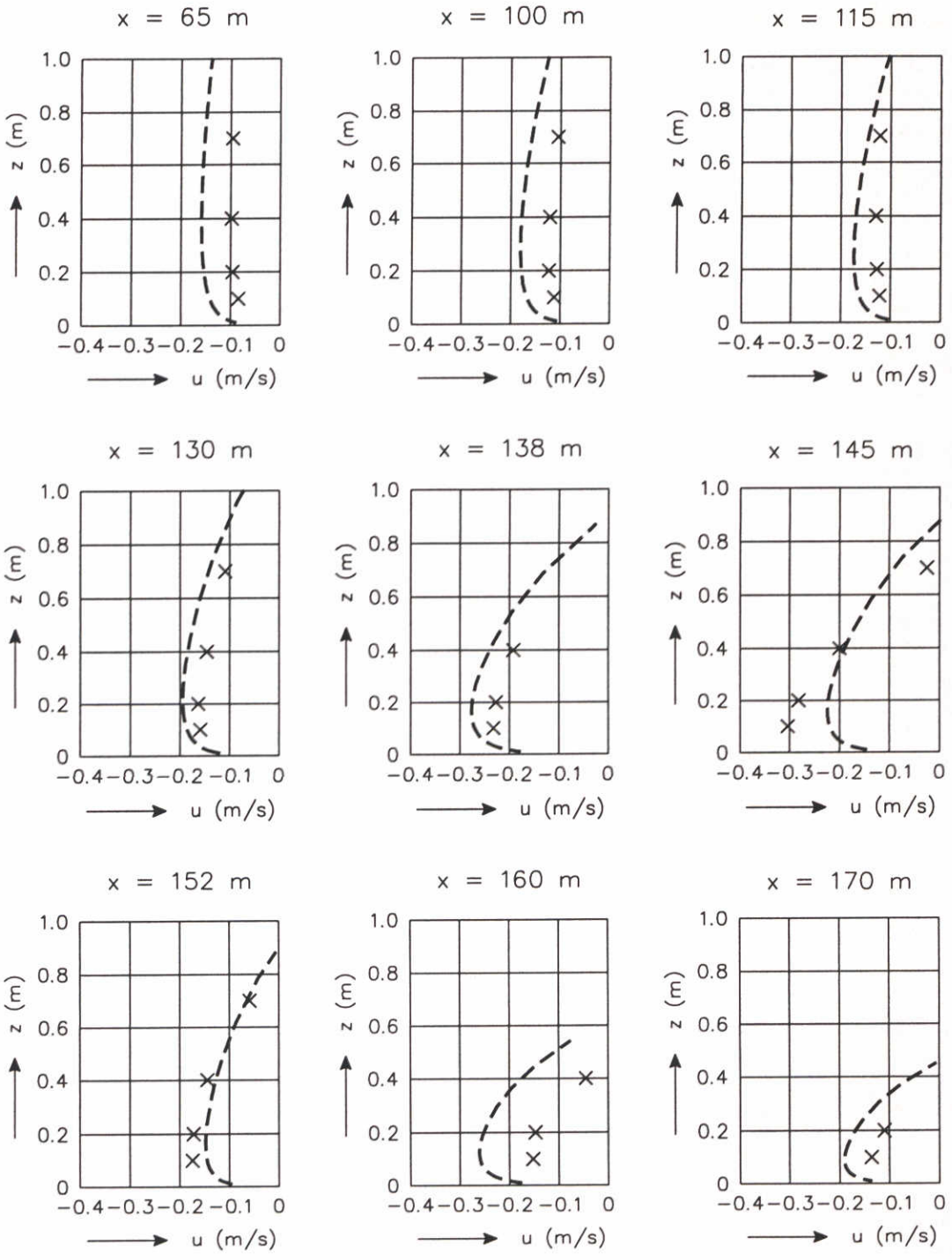

RETURN FLOW

DELFT HYDRAULICS | H 2129 | FIG. 4.3

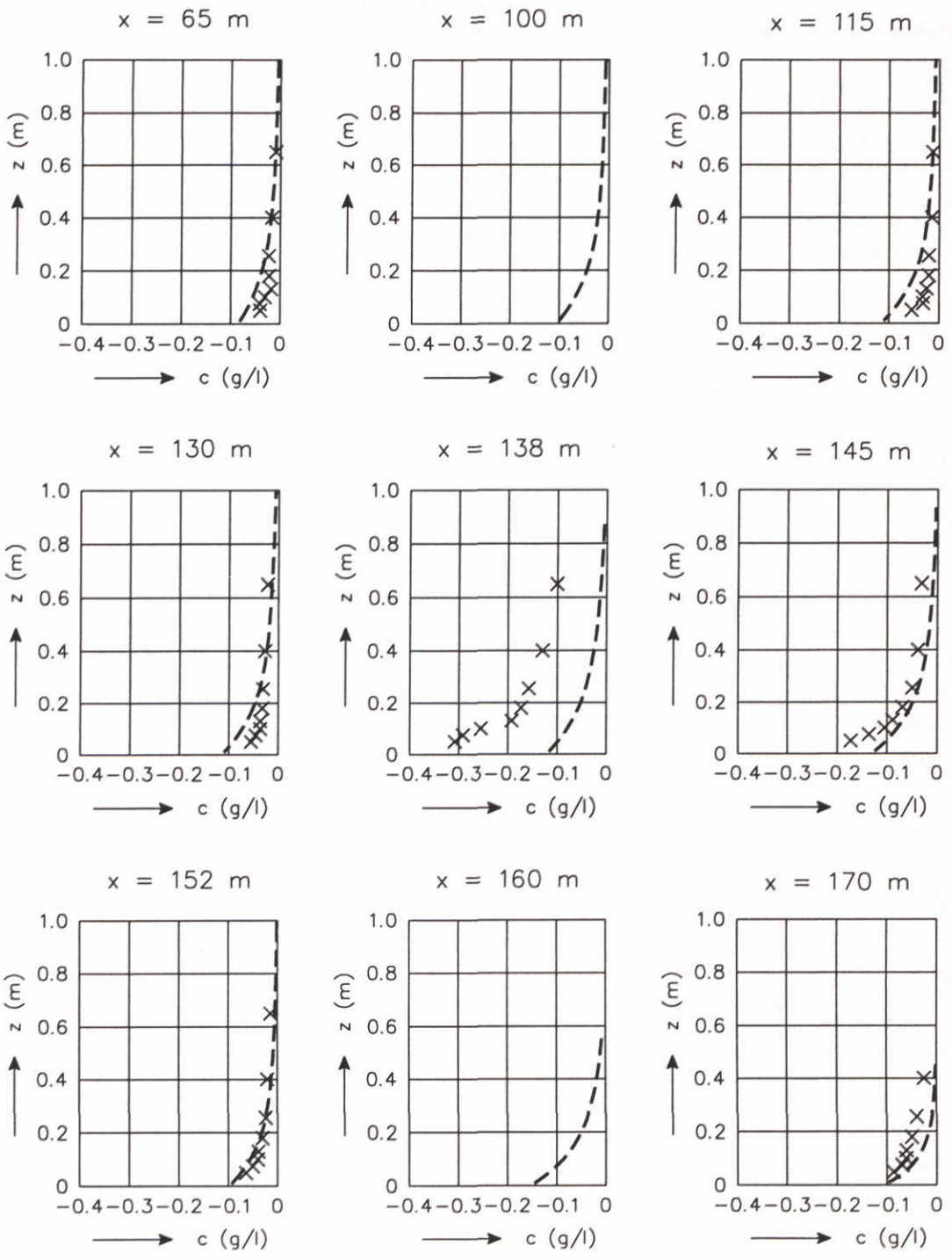

SEDIMENT CONCENTRATION

DELFT HYDRAULICS | H 2129 | FIG. 4.4

Appendix A

Example of input file

```
RUNIDENTIFICATIE        (lees in uni_tc.for)        (file demox.da
    208
GRID
    X_BEGIN NDX
     0.0   3
    NUMBER  DX        (total number < 119)
    25     4.
    10     2.
    80     1.
RUNPARAMETERS                (lees in inpx.dat)
       DT(day) NT   JCLOSE(-1,1,2) USTRA(m3/h)   JFR     IBOD     TDR
       1.0     0    -1              0.0          1       0        40.
7 DUMMY VALUES, FACVISC
       1.      1.       1.       1.      1.      1.       1.      0.1
COEFFICIENTS WAVES  AND FLOW
       GAMMA   ALFAC   FWEE    RKVAL   DIEPV   REMLAAG  BETD
       0.0     1.0     0.01     0.01    5.0     0.10      .1
COEFFICIENTS VELOCITIES AND TRANSPORTS
       D50      D90      DSS      RC      RW   PHILAT  DRHODX  DRHODY
       .19e-3   .3e-3    .16e-3   .01     .0    52.0    0.0     0.0
       TEMP    SALIN   C_R
       10.0     0.      .25
RANDVOORWAARDEN         (9 rvw-functies in deze volgorde)
       FUNCTION    CODE    VALUE   COLUMN  FILE
       'HO    '    1       4.0667  0       ' '
       'V_TIDE'    1       0.0     0       ' '
       'A_WAVE'    1       0.0     0       ' '
       'HRMS  '    1       .9579   0       ' '
       'T     '    1       5.0     0       ' '
       'Z     '    2       0.0     1       '%1b08mc.dat'
       'Z_FIX '    1      -30.0    0       ' '
       'V_WIND'    1       0.0     0       ' '
       'A_WIND'    1       20.0    0       ' '
BASICFUNCTIONS                  (lees in outfil.for)
      X-POINTS FOR TIMEFUNCTIONS (COLUMNS ON UTC###.HIS)
      2
      NR   X-POINT
      1    160.000
      2    170.000
NUMBER OF ACTUAL TIMEFUNCTIONS
      2
      FUNC  1  2                  (FUNC 1:29)
      1     1  1
      2     0  1
      T-POINTS FOR PLACE-FUNCTIONS (BLOCKS ON UTC###.MP@)
      1
      NR   T_POINT
      1      1.0
```

```
NUMBER OF ACTUAL PLACE FUNCTIONS
        10
        FUNC       @  1  2  3  4  5  6        (FUNC 1:29)
        1          1  1
        2          1  1
        3          1  1
        15         1  1
        16         1  1
        17         1  1
        18         1  1
        22         1  1
        24         1  1
        26         1  1
VOLUMINA
        2
        X1              X2                H
        88.000000       138.000000        -5.000000
        138.000000      188.000000        -3.000000
VERT.FUNCTIONS
        9
        X_POINT      T_POINT      F-TYPE (1=Z, 2=T, 3=BOTH)
         65.0       1.0          1
        100.0       1.0          1
        115.0       1.0          1
        130.0       1.0          1
        138.0       1.0          1
        142.0       1.0          1
        152.0       1.0          1
        160.0       1.0          1
        170.0       1.0          1
```

Appendix B

Demo of standard input file for bottom profile

```
1
0.00
   x(m)   z(m)
 19.00   .007
 19.50   .016
 20.00   .038
 20.50   .057
 21.00   .099
 21.50   .117
 22.00   .134
 22.50   .154
 23.00   .168
   .      .
   .      .
   .      .
191.50  5.200
192.00  5.230
```

where:

'1' represents the number of columns minus 1.
'0.00' represents the length of a cycle in case input is intended to be periodic (in case of time series)

In case of time series the first column is replaced by the time in days.

Appendix C

Integration of velocity profile

The vertical velocity gradient is given by:

$$\frac{\partial u_i}{\partial \sigma} = \frac{h}{\rho \phi_s \overline{\nu_t}} \left(\frac{(\tau_{s,i} - R_i) + R_i \sigma}{\sigma(\sigma_s - \sigma)} \right) \qquad ,\sigma > \delta \qquad \text{(C.1a)}$$

$$\frac{\partial u_i}{\partial \sigma} = \frac{h}{\rho \phi_s \overline{\nu_t}} \left(\frac{(\tau_{s,i} - R_i + \frac{D_f k_i}{\omega}) + (R_i - \frac{D_f k_i}{\delta\, \omega}) \sigma}{\sigma(\sigma_s - \sigma)} \right) \qquad ,\sigma < \delta \qquad \text{(C.1b)}$$

or:

$$\frac{\partial u_i}{\partial \sigma} = A \left(\frac{B_i + C_i \sigma}{\sigma(\sigma_s - \sigma)} \right) \qquad ,\sigma > \delta \qquad \text{(C.2a)}$$

$$\frac{\partial u_i}{\partial \sigma} = A_b \left(\frac{B_{b,i} + C_{b,i} \sigma}{\sigma(\sigma_b - \sigma)} \right) \qquad ,\sigma < \delta \qquad \text{(C.2b)}$$

where:

$$A = \frac{h}{\rho \phi_s \overline{\nu_t}},\ B_i = \tau_{s,i} - R_i \text{ and } C_i = R_i \qquad \text{(C.3a)}$$

$$A_b = \frac{h}{\rho (\phi \nu)_b},\ B_i = \tau_{s,i} - R_i + \frac{D_f k_i}{\omega} \text{ and } C_i = R_i - \frac{D_f k_i}{\omega} \qquad \text{(C.3b)}$$

This can be written as:

$$\frac{\partial u_i}{\partial \sigma} = A \left(\frac{B_i}{\sigma_s \sigma} + \frac{B_i/\sigma_s + C_i}{\sigma_s - \sigma} \right) \qquad ,\sigma > \delta \qquad \text{(C.4a)}$$

$$\frac{\partial u_i}{\partial \sigma} = A_b \left(\frac{B_{b,i}}{\sigma_b \sigma} + \frac{B_{b,i}/\sigma_b + C_{b,i}}{\sigma_b - \sigma} \right) \qquad ,\sigma > \delta \qquad \text{(C.4b)}$$

Given that $u_i = 0$ at $\sigma = \sigma_0$, the velocity in the bottom layer is now obtained by integration:

$$u_i = A_b \left(\frac{B_{b,i}}{\sigma_b} \ln \frac{\sigma}{\sigma_0} - (B_{b,i}/\sigma_b + C_{b,i}) \ln \frac{\sigma_b - \sigma}{\sigma_b - \sigma_0} \right) \qquad ,\sigma < \delta \qquad \text{(C.5)}$$

This equation is valid for $\sigma > e\sigma_0$; below this level, a linear velocity decay towards the bottom is assumed.

The contribution of these velocity components in the bottom layer to the depth-integrated follows from yet another integration:

$$\int_{\sigma_0}^{\delta} u_i \, d\sigma =$$

$$= A_b \left(\frac{B_{b,i}}{\sigma_b} (\sigma \ln \frac{\sigma}{\sigma_0} - \sigma) + (\frac{B_{b,i}}{\sigma_b} + C_{b,i}) \left((\sigma_b - \sigma) \ln \frac{\sigma_b - \sigma}{\sigma_b - \sigma_0} + \sigma \right) \right)_{\sigma_0}^{\delta}$$

$$= A_b \left(\frac{B_{b,i}}{\sigma_b} (\ln \frac{\delta}{\sigma_0} - (\delta - \sigma_0)) + (\frac{B_{b,i}}{\sigma_b} + C_{b,i}) \left((\sigma_b - \delta) \ln \frac{\sigma_b - \delta}{\sigma_b - \sigma_0} + (\delta - \sigma_0) \right) \right)$$

$$= \frac{A_b}{\sigma_b} \left(\ln \frac{\delta}{\sigma_0} + (\sigma_b - \delta) \ln \frac{\sigma_b - \delta}{\sigma_b - \sigma_0} \right) B_{b,i} + A_b \left((\sigma_b - \delta) \ln \frac{\sigma_b - \delta}{\sigma_b - \sigma_0} + (\delta - \sigma_0) \right) C_{b,i} \qquad \text{(C.6)}$$

The velocity at the top of the bottom layer is given by:

$$u_{\delta,i} = A_b \left(\frac{B_{b,i}}{\sigma_b} \ln \frac{\delta}{\sigma_0} - (B_{b,i}/\sigma_b + C_{b,i}) \ln \frac{\sigma_b - \delta}{\sigma_b - \sigma_0} \right) \qquad \text{(C.7)}$$

This velocity is the lower boundary condition for the middle layer. In this layer, we have:

$$u_i = u_{\delta,i} + A \left(\frac{B_i}{\sigma_s} \ln \frac{\sigma}{\delta} - (B_i/\sigma_s + C_i) \ln \frac{\sigma_s - \sigma}{\sigma_s - \delta} \right) \qquad ,\sigma > \delta \qquad \text{(C.8)}$$

The contribution of the middle layer to the depth-integrated flow is:

$$\int_{\delta}^{1} u_i \, d\sigma =$$

$$= u_{\delta,i}(1-\delta) + A \left(\frac{B_i}{\sigma_s} (\sigma \ln \frac{\sigma}{\delta} - \sigma) + (\frac{B_i}{\sigma_s} + C_i) \left((\sigma_s - \sigma) \ln \frac{\sigma_s - \sigma}{\sigma_s - \delta} + \sigma \right) \right)_{\delta}^{1}$$

$$= u_{\delta,i}(1-\delta) + A \left(\frac{B_i}{\sigma_s} (\ln \frac{1}{\delta} - (1-\delta)) + (\frac{B_i}{\sigma_s} + C_i) \left((\sigma_s - 1) \ln \frac{\sigma_s - 1}{\sigma_s - \delta} + (1-\delta) \right) \right) \qquad \text{(C.9)}$$

The depth-mean velocity components are given by:

$$\int_{\sigma_0}^{1} u_i \, d\sigma = \int_{\sigma_0}^{\delta} u_i \, d\sigma + \int_{\delta}^{1} u_i \, d\sigma =$$

$$= \frac{A_b}{\sigma_b} \left(\delta \ln \frac{\delta}{\sigma_0} + (\sigma_b - \delta) \ln \frac{\sigma_b - \delta}{\sigma_b - \sigma_0} \right) B_{b,i} + A_b \left((\sigma_b - \delta) \ln \frac{\sigma_b - \delta}{\sigma_b - \sigma_0} + (\delta - \sigma_0) \right) C_{b,i} +$$

$$+\frac{A_b}{\sigma_b}\left((1-\delta)\ln\frac{\delta}{\sigma_0}-(1-\delta)\ln\frac{\sigma_b-\delta}{\sigma_b-\sigma_0}\right)B_{b,i} - A_b\left((1-\delta)\ln\frac{\sigma_b-\delta}{\sigma_b-\sigma_0}\right)C_{b,i} +$$

$$+\frac{A}{\sigma_s}\left(\ln\frac{1}{\delta}+(\sigma_s-1)\ln\frac{\sigma_s-1}{\sigma_s-\delta}\right)B_i + A\left((\sigma_s-1)\ln\frac{\sigma_s-1}{\sigma_s-\delta}+(1-\delta)\right)C_i =$$

$$=\frac{A_b}{\sigma_b}\left(\ln\frac{\delta}{\sigma_0}+(\sigma_b-1)\ln\frac{\sigma_b-\delta}{\sigma_b-\sigma_0}\right)B_{b,i} + A_b\left((\sigma_b-1)\ln\frac{\sigma_b-\delta}{\sigma_b-\sigma_0}+(\delta-\sigma_0)\right)C_{b,i} +$$

$$+\frac{A}{\sigma_s}\left(\ln\frac{1}{\delta}+(\sigma_s-1)\ln\frac{\sigma_s-1}{\sigma_s-\delta}\right)B_i + A\left((\sigma_s-1)\ln\frac{\sigma_s-1}{\sigma_s-\delta}+(1-\delta)\right)C_i \qquad \text{(C.10)}$$

So:

$$\overline{u_i} = G_b\,B_{b,i} + H_b\,C_{b,i} + G\,B_i + H\,C_i \qquad \text{(C.11)}$$

We now have obtained a direct relation between the mean velocity u_i, the depth-independent forcing R_i, the surface shear stress $\tau_{s,i}$ and streaming term $(D_f k_i)/\omega$:

$$\overline{u_i} = (H_b+H-G_b-G)\,R_i + (G_b+G)\,\tau_{s,i} + (G_b-\frac{H_b}{\delta})\frac{D_f k_i}{\omega} \qquad \text{(C.12)}$$

In the longshore direction, we can now solve the depth-averaged velocity for a given forcing R_y and surface shear stress $\tau_{s,y}$. In cross-shore direction, the equation is used to solve the unknown forcing (pressure gradient) R_x from the known mean cross-shore velocity and the surface shear stress component $\tau_{s,x}$.

Having solved B_i and C_i we can now compute the vertical distribution of the velocity components in x- and y-direction.

main office
Rotterdamseweg 185
p.o. box 177
2600 MH Delft
The Netherlands
telephone (31) 15 - 56 93 53
telefax (31) 15 - 61 96 74
telex 38176 hydel-nl

location 'De Voorst'
Voorsterweg 28, Marknesse
p.o. box 152
8300 AD Emmeloord
The Netherlands
telephone (31) 5274 - 29 22
telefax (31) 5274 - 35 73
telex 42290 hylvo-nl